

Going chiral: overlap versus twisted mass fermions

W. Bietenholz¹, S. Capitani², T. Chiarappa³, N. Christian^{3,4},
M. Hasenbusch⁵, K. Jansen³, K.-I. Nagai³, M. Papinutto³,
L. Scorzato¹, S. Shcheredin¹, A. Shindler³, C. Urbach^{3,4},
U. Wenger³ and I. Wetzorke³

Collaboration

¹ Institut für Physik, Humboldt Universität zu Berlin
Newtonstr. 15, D-12489 Berlin, Germany

² Institut für Physik/Theoretische Physik
Universität Graz, A-8010 Graz, Austria

³ NIC/DESY Zeuthen
Platanenallee 6, D-15738 Zeuthen, Germany

⁴ Institut für Theoretische Physik, Freie Universität Berlin
Arnimallee 14, D-14195 Berlin, Germany

⁵ Dipartimento di Fisica, Università di Pisa
Via Buonarroti 2, I-56127 Pisa, Italy

Abstract

We compare the behavior of overlap fermions, which are chirally invariant, and of Wilson twisted mass fermions at full twist in the approach to the chiral limit. Our quenched simulations reveal that with both formulations of lattice fermions pion masses of $\mathcal{O}(250 \text{ MeV})$ can be reached in practical applications. Our comparison is done at a fixed value of the lattice spacing $a \simeq 0.123 \text{ fm}$. A number of quantities are measured such as hadron masses, pseudoscalar decay constants and quark masses obtained from Ward identities. We also determine the axial vector renormalization constants in the case of overlap fermions.

1 Introduction

Approaching the so-called physical point in lattice QCD, where the light meson masses assume their values observed in nature, is a major challenge for numerical simulations in lattice field theory. In this regime of QCD, where the light quarks, i.e. the u and d flavors, play the dominant role, the explicit breaking of chirality on the lattice, the role of topological charge excitations and the appearance of unphysical very-low lying eigenvalues of the lattice Dirac operator can render simulations very demanding, if not impossible.

The complicated low energy dynamics of light quarks of the fundamental theory can be effectively described by *chiral perturbation theory* [1]. In chiral perturbation theory (χ PT) an effective Lagrangian is constructed with terms that are compatible with the global symmetries of the original QCD Lagrangian and that are ordered according to some hierarchy, which depends on the expansion regime. In this effective Lagrangian, each term has a coefficient which enters as a free parameter that cannot be determined within the chiral perturbation theory itself. Such coefficients are denoted as the *low energy constants*, and they play a vital role in many QCD processes at low energy. The challenge is then to determine these low energy constants from first principles, i.e. directly from QCD as the underlying, fundamental theory.

Such a link between the effective theory and fundamental QCD can, in principle, be provided by lattice techniques. However, simulations at values of quark masses, where such a contact to χ PT can safely be made, are very difficult, as mentioned above. Standard approaches using the Wilson fermion discretization of lattice QCD are confronted with technical algorithmic problems since in this case the bare quark mass does not provide an infrared regulator. In this paper we will consider two formulations of lattice QCD that are able to overcome this problem: overlap fermions [2] and twisted mass fermions [3]. In particular, we will concentrate on the Wilson twisted mass (Wtm) [4] formulation of lattice fermions at a full twisting angle of $\pi/2$. Both, overlap and Wtm fermions lead to $\mathcal{O}(a)$ improvement for physical quantities and are expected to allow for simulations at very small quark masses, corresponding to their physical values as estimated from experiment. Overlap fermions induce an exact lattice chiral symmetry [5] and provide a sound definition of the topological charge [6]. Hence they have conceptual advantages, but they are, unfortunately, rather expensive in numerical simulations. Twisted mass fermions on the other hand are rather cheap to simulate but show residual chiral symmetry breaking effects. Hence it is not clear how the benefits of both formulations of lattice QCD compare in practical simulations and here we would like to give a first direct comparison.

We compute a number of quantities, Ward identity quark masses, meson and baryon masses, decay constants and renormalization factors, driving the values of quark masses small enough that χ PT is expected to be applicable. While for Wtm fermions this is the first work along this line, we refer to Refs. [7] for other simulations in the p -regime of chiral perturbation theory in the case of overlap fermions.

We emphasize that the present comparison between both lattice fermions is only performed in the quenched approximation at $\beta = 5.85$, corresponding to a lattice spacing of $a \simeq 0.123$ fm. No attempt of a scaling analysis is performed here, see however Ref. [8] for a first work in this direction for Wtm. It is the main goal of this paper to investigate how both formulations of lattice QCD behave in their approach to the chiral limit. In particular we are aiming at an investigation to how small quark masses both formulations can be driven when used in practical simulations.

We will also provide a computing time estimate from our results in Ref. [9]. This question is most important for eventual dynamical simulations. If, for many quantities, Wilson twisted mass fermions can reach quark masses that can be compared with overlap fermions, their advantage in the simulation cost will immediately benefit in dynamical simulations. For first results of dynamical twisted mass fermions, see Ref. [10].

2 Overlap and Wilson twisted mass fermions

In this section we discuss the two fermion formulations of lattice QCD that we have employed to study the approach to the chiral limit at small values of the quark mass: overlap fermions and Wilson twisted mass fermions. We emphasize some relevant points for the present work and refer to Refs. [11, 12] for further discussions.

2.1 Overlap fermions

Over the last few years a lattice fermion formulation leading to an exact lattice chiral symmetry was elaborated, namely the *Ginsparg-Wilson fermions*. The corresponding lattice Dirac operator D_{GW} satisfies the Ginsparg-Wilson relation [13]

$$D_{\text{GW}}\gamma_5 + \gamma_5 D_{\text{GW}} = 2aD_{\text{GW}}\gamma_5 R D_{\text{GW}} , \quad (1)$$

where R is a local term. The realization of an operator D_{GW} that we use here is the overlap fermion, which is characterized by the Neuberger-Dirac operator [2]. For $R_{xy} = \delta_{xy}/(2\rho)$ it takes the form

$$\begin{aligned} D_{\text{ov}} &= \left(1 - \frac{m_{\text{ov}}\bar{a}}{2}\right) D_{\text{ov}}^{(0)} + m_{\text{ov}} , \\ D_{\text{ov}}^{(0)} &= \frac{1}{\bar{a}} \left\{1 + A/\sqrt{A^\dagger A}\right\} , \quad A = aD_{\text{W}} - \rho , \end{aligned} \quad (2)$$

where $\bar{a} \equiv a/\rho$ and D_{W} is the standard Wilson-Dirac operator,

$$D_{\text{W}} = \sum_{\mu=1}^4 \frac{1}{2} [\gamma_\mu (\nabla_\mu^* + \nabla_\mu) - a\nabla_\mu^* \nabla_\mu] . \quad (3)$$

∇_μ and ∇_μ^* denote the usual forward and backward covariant lattice derivatives, m_{ov} is the bare quark mass and $\rho \gtrsim 1$ is a mass parameter, which we set to 1.6.

$D_{\text{ov}}^{(0)}$ (the overlap operator at zero quark mass) obeys the Ginsparg-Wilson relation in Eq. (1). It does obey a lattice modified but exact chiral symmetry, which turns into the standard chiral symmetry in the continuum limit [5]. This symmetry protects the lattice fermion from additive mass renormalization and from $\mathcal{O}(a)$ lattice artifacts, i.e. the action built by the operator in Eq. (2) is $\mathcal{O}(a)$ improved. It also implies that there are exact zero modes with a definite chirality [6]. Thus the topological charge can be identified as the index obtained from these zero modes. $\mathcal{O}(a)$ improved bilinears are constructed as follows:

$$O_{\Gamma}^{\text{ov}} = \bar{\psi}^{\alpha} \Gamma \left(1 - \frac{\bar{a} D_{\text{ov}}^{(0)}}{2} \right) \psi^{\beta} = \frac{1}{1 - \frac{\bar{a} m_{\beta}}{2}} (\bar{\psi}^{\alpha} \Gamma \psi^{\beta}) \quad (4)$$

where ψ^{α} and ψ^{β} are two different flavours, and the last equality holds for correlation functions at non-zero physical distance. In the following we will use the following notation: $O_{\gamma_5}^{\text{ov}} \equiv P$, $O_{\Gamma}^{\text{ov}} \equiv S$, $O_{\gamma_{\mu}}^{\text{ov}} \equiv V_{\mu}$ and $O_{\gamma_{\mu} \gamma_5}^{\text{ov}} \equiv A_{\mu}$.

By now the overlap fermion has a very well established theoretical basis, but its simulation is rather tedious. In our code the inverse square root is approximated by Chebyshev polynomials to an absolute accuracy of 10^{-15} (see Ref. [9] for details). On this level of precision the lattice chiral symmetry is certainly reliable. Unfortunately the computational effort exceeds the one for Wtm by a large amount, which means that, at least for large volumes, for the time being only *quenched* QCD simulations are possible with Ginsparg-Wilson fermions, at least when chiral symmetry is to be realized to the precision enforced in this paper. The virtues of this formulation include also a protection against exceptional configurations, thus allowing simulations at small pion masses, certainly when they are comparable or larger than their physical values.

2.2 Wilson twisted mass fermions

As an alternative to regulate exceptionally small eigenvalues, Wilson fermions with a *twisted mass* [3, 4] can be used. This means that the Wilson-Dirac operator obtains a mass term of the form

$$m_{\text{tm}} + i\mu\gamma_5\tau^3, \quad (5)$$

where m_{tm} is again the bare quark mass, τ^b are the usual Pauli matrices acting in flavor space and μ is the “twisted mass”.

In this paper we will work with Wilson twisted mass fermions that can be arranged to be $\mathcal{O}(a)$ improved without additional improvement terms. To be more precise, let us start by writing the Wtm QCD action (in the twisted basis) as

$$S[U, \psi, \bar{\psi}] = a^4 \sum_x \bar{\psi}(x) (D_W + m_{\text{tm}} + i\mu\gamma_5\tau^3) \psi(x), \quad (6)$$

where the operator D_W is given in Eq. (3).

The action as it stands in Eq. (6) can, of course, be studied in the full parameter space (m_{tm}, μ) . A special case arises, however, when m_{tm} is tuned towards a critical bare quark mass m_c . In this, and only in this situation, all physical quantities are (or can easily be) $\mathcal{O}(a)$ improved. It is hence natural to rewrite

$$m_{\text{tm}} = m_c + \tilde{m} \quad (7)$$

with \tilde{m} an offset quark mass. The values of m_c need only to be known with $\mathcal{O}(a)$ accuracy [4] and can be, for instance, taken from the pure Wilson theory at $\mu = 0$.

In this approach there is no need of improving the operators, so we will consider the usual local bilinears

$$\begin{aligned} P^b &= \bar{\psi} \gamma_5 \frac{\tau^b}{2} \psi & S^b &= \bar{\psi} \frac{\tau^b}{2} \psi \\ A_\mu^b &= \bar{\psi} \gamma_\mu \gamma_5 \frac{\tau^b}{2} \psi & V_\mu^b &= \bar{\psi} \gamma_\mu \frac{\tau^b}{2} \psi \end{aligned} \quad (8)$$

where b is a $SU(2)$ flavour index.

Of particular interest is the PCVC relation. In the twisted basis it takes the form

$$\partial_\mu^* V_\mu^b = -2\mu \epsilon^{3bc} P^c, \quad (9)$$

where ∂_μ^* is the lattice backward derivative. Through a vector variation of the action one obtains the point-split vector current as defined in Ref. [3]. This current is protected against renormalization and using the point-split vector current, the PCVC relation is an exact lattice identity. This implies that $Z_P = Z_\mu^{-1}$, where Z_μ is the renormalization constant for the twisted mass μ . This will become important in the extraction of the pseudoscalar decay constant f_π as described below. Recent tests have revealed a very promising scaling behavior of this lattice fermion formulation (in quenched simulations) [8].

3 Numerical results

Using standard heat bath and over-relaxation techniques to generate gauge field configurations with the Wilson plaquette action, we have performed various simulations at $\beta = 5.85$, which corresponds to a value of the lattice spacing $a \simeq 0.123$ fm ($a^{-1} \simeq 1.605$ GeV using $r_0 = 0.5$ fm [14]). Periodic boundary conditions were used in this work.

For overlap fermions we have 140 configurations on a $12^3 \times 24$ lattice ($L_{12} \sim 1.48$ fm). The bare quark masses are $m_{\text{ov}} a = 0.01, 0.02, 0.04, 0.06, 0.08, 0.10$. The simulations for twisted mass fermions are done at full twist. This is achieved by choosing $m_{\text{tm}} = m_c$ in the pure Wilson theory at $\mu = 0$. In the standard hopping parameter κ notation the offset quark mass is related to κ by $\tilde{m} = \frac{1}{2\kappa} - \frac{1}{2\kappa_c}$. Choosing $m_{\text{tm}} = m_c$ then corresponds to use $\kappa = \kappa_c = 0.16166(2)$ from the vanishing of

the pion mass for Wilson fermions [8]. The twisted quark mass parameter was chosen to be $\mu a = 0.005, 0.01, 0.02, 0.04, 0.06, 0.08, 0.10$. We then accumulated 140 configurations on $12^3 \times 24$, 140 configurations on $14^3 \times 32$ ($L_{14} \sim 1.72$ fm) and 380 configurations on $16^3 \times 32$ ($L_{16} \sim 1.97$ fm) lattices. In tables and plots below both m_{ov} and μ are called m_{bare} .

Our simulations, performed at a number of bare quark mass values, applied a multiple mass solver (MMS) in both cases. The MMS for twisted mass fermions will be described in a forthcoming paper [9], whereas the MMS for the usual fermion formulations can be found in Ref. [15]. In order to improve the projection on the fundamental states of our correlators, we have implemented the Jacobi smearing in the way it is described in Refs. [16, 17].

In the following we will extract several physical quantities (hadron masses and decay constants) using the overlap and the Wtm formulation of lattice QCD. Since the flavor structure of the quark propagators is important in the Wtm case, we will specify the flavor content of the local operators only for this formulation. We will indicate the fermionic action used in order to distinguish the correlation functions, where necessary, of the two formulations.

3.1 Meson masses

The first quantities we compared are the meson masses M_{meson} . They are extracted by fitting the suitable two-point correlation functions to the standard expression obtained from a spectral decomposition and retaining only the fundamental state ($a \ll x_0 \ll T$)

$$a^3 \sum_{\vec{x}} \langle O^\dagger(\vec{x}, x_0) O(0) \rangle = \frac{|\langle 0 | O | \text{meson} \rangle|^2}{M_{\text{meson}}} e^{-M_{\text{meson}} \frac{T}{2}} \cosh \left[M_{\text{meson}} \left(x_0 - \frac{T}{2} \right) \right] \quad (10)$$

in the time interval $[t_{\text{min}}, \frac{T}{2}]$ (with $a \ll t_{\text{min}} < \frac{T}{2}$). t_{min} has been chosen by considering the effective mass, the dependence of the fit on t_{min} and by comparing with a two-state fit. We extract the pseudoscalar masses (both degenerate and non-degenerate) from the correlation functions

$$C_{P,\text{tm}}^b(x_0) = a^3 \sum_{\vec{x}} \langle P^b(\vec{x}, x_0) P^b(0) \rangle_{\text{tm}}, \quad b = 1, 2. \quad (11)$$

For overlap fermions we consider

$$C_{P,\text{ov}}(x_0) = a^3 \sum_{\vec{x}} \langle P^\dagger(\vec{x}, x_0) P(0) \rangle_{\text{ov}}, \quad (12)$$

and

$$C_{P-S,\text{ov}}(x_0) = a^3 \sum_{\vec{x}} \langle P^\dagger(\vec{x}, x_0) P(0) - S^\dagger(\vec{x}, x_0) S(0) \rangle_{\text{ov}}, \quad (13)$$

$m_{\text{bare}}a$	$M_{\pi,\text{ov}}^P a$	$M_{\pi,\text{ov}}^{P-S} a$	$M_{\pi,\text{tm}}^{12^3 \times 24} a$	$M_{\pi,\text{tm}}^{14^3 \times 32} a$	$M_{\pi,\text{tm}}^{16^3 \times 32} a$	$M_{\pi,\text{tm}}^{16^3 \times 32} L_{16}$
0.005	-	-	-	-	0.1700(25)	2.7
0.01	0.212(9)	0.140(20)	0.2327(70)	0.2301(37)	0.2254(19)	3.6
0.02	0.237(7)	0.196(14)	0.3193(48)	0.3175(30)	0.3122(16)	5.0
0.04	0.299(5)	0.280(10)	0.4520(40)	0.4506(23)	0.4452(14)	7.1
0.06	0.355(4)	0.346(8)	0.5596(35)	0.5575(19)	0.5535(12)	8.9
0.08	0.405(4)	0.401(7)	0.6541(31)	0.6510(17)	0.6488(11)	10.4
0.10	0.450(4)	0.451(6)	0.7417(26)	0.7378(16)	0.7359(11)	11.8

Table 1: We show numerical results for the pion masses obtained with overlap fermions using both the correlators $C_{P,\text{ov}}$ and, $C_{P-S,\text{ov}}$, and with Wtm fermions using three different volumes. The overlap results were obtained on a $12^3 \times 24$ lattice, and we set $\beta = 5.85$ everywhere. The bare quark mass m_{bare} corresponds to m_{ov} in the overlap and to μ in the twisted mass case.

where the contribution of the topological zero modes cancels [18, 7]. This last method has the drawback that the scalar meson appears as an excited state and can affect the extraction of the mass of the ground state for large quark masses. In our study, however, the quark masses are sufficiently small such that this problem never occurs.

In Figure 1 and Tables 1, 2 we give an overview of our results for the pseudoscalar meson masses. For twisted mass fermions we have performed simulations on three volumes, such that we can investigate finite volume effects. On the $12^3 \times 24$ lattice, for the largest bare quark masses there are small contaminations from the excited states (which include also states of opposite parity appearing as $\mathcal{O}(a^2)$ artifacts) which are removed by using sink-smearred correlators. Apart from this effect, small finite volume effects are visible at the smallest masses. An analysis along the lines of Ref. [19] shows that, on the pion masses corresponding to smallest value of $M_\pi L$ (i.e. those corresponding to $\mu a = 0.01$ for $L = L_{12}$ and to $\mu a = 0.005$ for $L = L_{16}$), the finite volume effects are within 2-3 percent and at most within two standard

$m_{\text{bare}}a$	$M_{\pi,\text{ov}}^{P-S} a$	$M_{\pi,\text{ov}}^{P-S} L_{12}$	$M_{\pi,\text{tm}}^{12^3 \times 24} a$	$M_{\pi,\text{tm}}^{14^3 \times 32} a$	$M_{\pi,\text{tm}}^{16^3 \times 32} a$
0.01	0.134(22)	1.6	0.2332(70)	0.2303(39)	0.2257(21)
0.02	0.192(16)	2.3	0.3203(49)	0.3172(28)	0.3126(18)
0.04	0.275(12)	3.4	0.4523(41)	0.4493(22)	0.4455(16)
0.06	0.342(10)	4.2	0.5584(38)	0.5564(20)	0.5538(14)
0.08	0.397(10)	4.8	0.6510(36)	0.6504(19)	0.6492(13)
0.10	0.448(8)	5.4	0.7353(35)	0.7363(18)	0.7361(13)

Table 2: The same as Table 1 but with sink smearing.

deviations from the extrapolated infinite volume limit. In practice they are thus not really relevant for the following discussion. Below, we will present only those Wtm results which were obtained on the $16^3 \times 32$ lattice, for which finite volume effects are completely negligible as long as μa is larger than 0.005.

The problem of isolating the ground state does not appear in the overlap case when we analyze the $C_{P,ov}(x_0)$ correlator. Even when we introduce a parity violating term explicitly with the $C_{P-S,ov}(x_0)$ correlator, we still do not have any problem to extract the pion mass for all the values of the quark masses simulated. This is due to the fact that, at a fixed value of the bare quark mass, the pseudoscalar masses are smaller (and the gap between the fundamental and the excited states in the pseudoscalar correlator or between the fundamental state of the pseudoscalar and of the scalar correlators larger) than the corresponding masses for Wtm.

Given the value of $M_\pi L$ in the case of overlap fermions and the experience from Wtm fermions, we expect very small finite volume effects for the 5 heaviest quark masses (at the level of few percents in the case of $m_{ov} a = 0.02$). For the lowest quark mass (for which $M_{\pi,ov} L = 1.6$) finite volume effects can be more relevant and thus we usually do not include the corresponding data point in the fits. However, the analysis of the various quantities presented below suggests that, for this quark mass, finite volume effects are not larger than our statistical error.

Note that for $\mathcal{O}(a)$ improved Wilson fermions results [20, 21], which are also shown in Figure 1, the simulations had to be stopped at rather large values of the quark mass to avoid the appearance of exceptional configurations. On the contrary, with both Wilson twisted mass fermions and overlap fermions we can reach very low values of the quark and hence of the pion mass.

For overlap fermions, the masses extracted from $C_{P-S,ov}(x_0)$ have, to a very good approximation, a linear behavior down to the smallest mass ($M_\pi \simeq 220$ MeV). A linear extrapolation to the chiral limit gives an intercept of $-0.002(6)$. For Wilson twisted mass fermions we have performed two fits: a linear one on the four smallest masses from which we get an intercept of $0.0017(2)$ with $\chi^2/d.o.f. = 1.35$, and a quadratic one on all of the 7 points from which we get an intercept of $0.0045(4)$ with $\chi^2/d.o.f. = 0.19$. As we can see, the data show a behavior which is much better described by a parabola than by a straight line. We attribute the value of the intercept, non-compatible with zero in the chiral limit, to the $\mathcal{O}(a)$ error in κ_c , which at $\mu = 0$ gives an $\mathcal{O}(a)$ residual pion mass. The dependence of M_π^2 upon μ and a at small values of the twisted mass can in principle be computed in χ PT with the inclusion of the twisted mass term [22]. The curvature of the Wtm data at high values of μ , absent for overlap fermions, can be explained by the uncertainty of $\mathcal{O}(a)$ in κ_c (determined in the pure Wilson case $\mu = 0$). This induces an uncertainty of $\mathcal{O}(a^2 \mu^2)$ in the pion mass, which increases with a higher value of the twisted mass.

We clearly observe that the pion masses obtained with twisted mass fermions shown in Figure 1 always lay above the ones from the simulations using overlap fermions. This suggests that the renormalization factor Z_m of the quark mass should be larger for Wilson twisted mass fermions when compared to overlap fermions. It

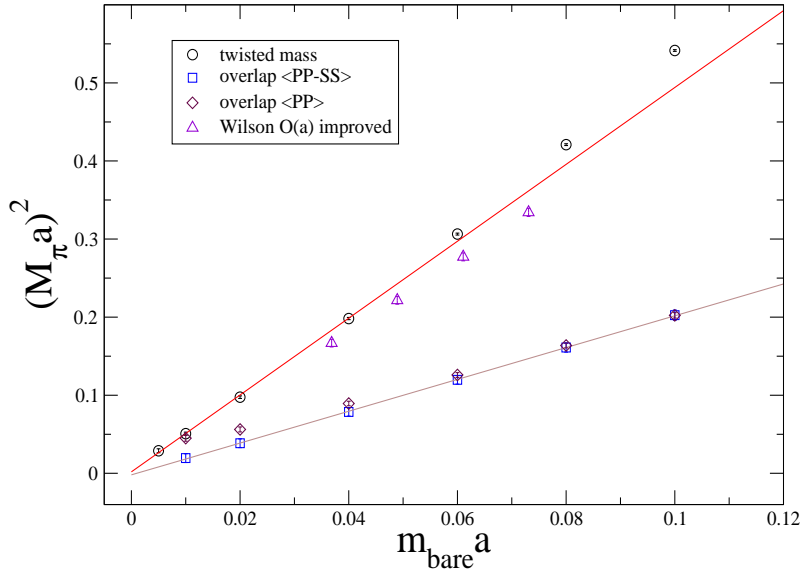


Figure 1: Comparison of quenched results for the pion mass squared as a function of the bare quark mass for three lattice fermions: standard $O(a)$ improved Wilson fermions [20, 21], twisted mass fermions and overlap fermions. The bare quark mass corresponds to m_{ov} in the overlap and to μ in the twisted mass case.

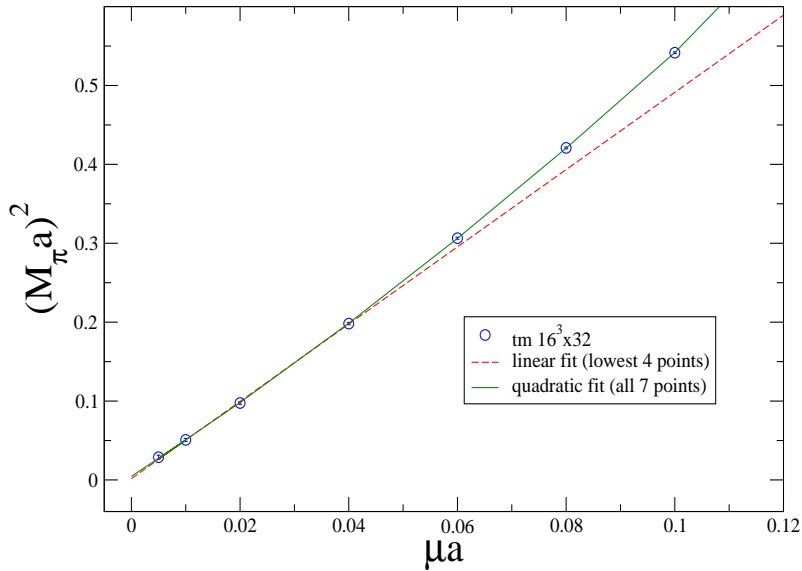


Figure 2: Twisted mass fermions: linear and quadratic fit of the squared pion masses as function of the bare quark mass.

$m_{\text{bare}}a$	$M_{\rho}^{\text{ov}}a$	$M_{\rho}^{\text{tm}}a$
0.005	-	0.356(48)
0.01	0.632(34)	0.468(46)
0.02	0.638(26)	0.543(24)
0.04	0.653(16)	0.6482(91)
0.06	0.666(12)	0.7333(57)
0.08	0.683(9)	0.8087(41)
0.10	0.702(8)	0.8799(33)

Table 3: *Vector meson masses with sink smearing.*

also means that smaller values of the quark mass have to be simulated with Wilson twisted mass fermions to reach the same pion mass as with overlap fermions.

As a next quantity we consider the *vector meson mass*. It has been extracted from the following correlators,

$$C_{A,\text{tm}}^b(x_0) = \frac{a^3}{3} \sum_{k=1}^3 \sum_{\vec{x}} \langle A_k^b(\vec{x}, x_0) A_k^b(0) \rangle_{\text{tm}}, \quad b = 1, 2,$$

$$C_{V,\text{ov}}(x_0) = \frac{a^3}{3} \sum_{k=1}^3 \sum_{\vec{x}} \langle V_k^\dagger(\vec{x}, x_0) V_k(0) \rangle_{\text{ov}}.$$

In order to extract a reliable value for the vector meson mass, sink-smearing has been used. For overlap data, where the volume is not so large and the statistical errors are consequently significant, the smearing procedure is important in order to isolate the ground state (at the same time reducing the statistical error of the estimated mass). For twisted mass data on the largest volume ($16^3 \times 32$), smearing has a small effect, apparently because it is not able to decrease substantially the coupling of the interpolating operators to the excited states. The vector meson mass has been extracted by averaging the values of the effective mass within a time interval which excludes the points at the largest times. This points are in fact affected by large statistical uncertainty and tend to lower the estimated value. The results are reported in Table 3 and plotted in Figure 3.

In the case of Wtm fermions, we report in Fig. 4 two examples for the plateaux of the effective mass of the vector meson, namely the case corresponding to the smallest quark mass $\mu a = 0.005$ (which has highest statistical fluctuations and for which we have chosen the plateau in the range $8 \leq x_0 \leq 13$) and that of an intermediate mass $\mu a = 0.06$ (with plateau chosen in the range $9 \leq x_0 \leq 12$). Despite the precautions described above, we still observe a strong decrease of the vector meson mass at low quark masses, as compared to the overlap case where the behavior with the pion mass squared is linear to a good approximation. We will discuss later, when

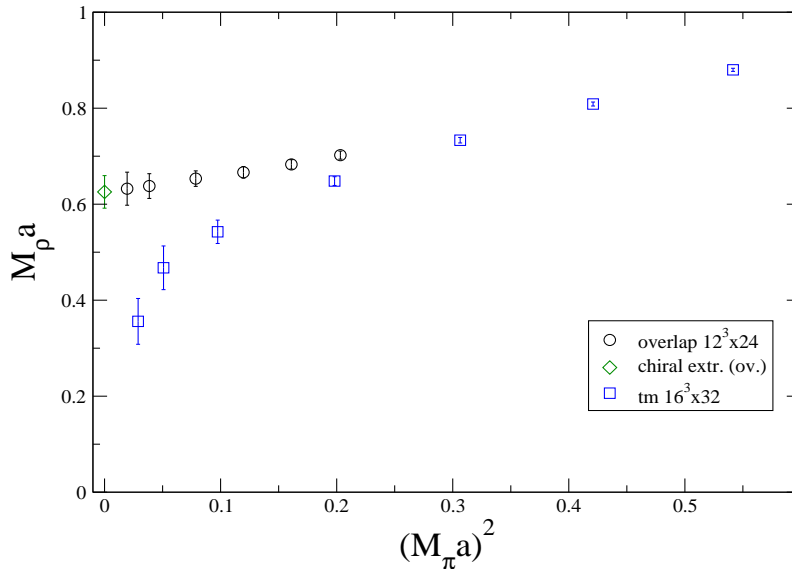


Figure 3: Comparison of results for the vector meson mass as a function of the pion mass squared for overlap and twisted mass fermions. The chiral extrapolation in the overlap case is done with a linear fit in M_π^2 .

examining f_π , the problems that can arise in the Wtm case when going down to low masses at fixed lattice spacing. This phenomenon has to be further investigated, for example by going to higher β values. This is beyond the scope of the present work and will be addressed in another (presently on-going) project whose ultimate goal is the study of the scaling behavior of various quantities in twisted mass QCD computed for a wide range of quark masses [23].

3.2 Renormalization constants

Using the method explained in Refs. [20, 21] we computed the renormalization group invariant (RGI) quark mass renormalization constant Z_m^{RGI} for Wtm and overlap fermions. Here we just describe the method and we refer to Refs. [20, 21] for a more detailed explanation. There are essentially two requirements for applying this method:

- Due to the symmetries of the lattice action, renormalization constants of different local operators are related in a simple way.
- Using an alternative discretization of QCD it is possible to compute a renormalized matrix element (or quark mass) in the continuum.

The basic idea is to compute a universal factor — that could be a RGI matrix element or quark mass — in the continuum at a fixed reference value of a physical

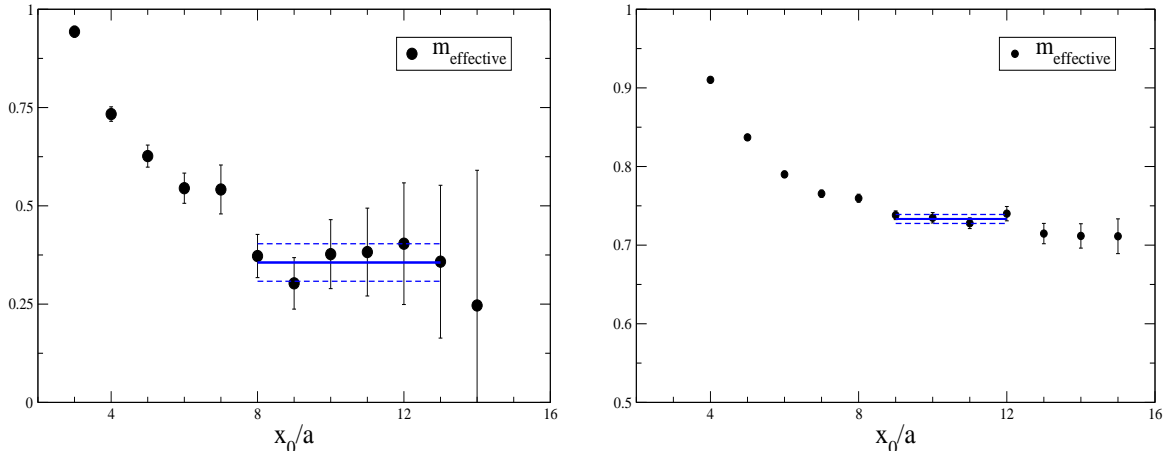


Figure 4: *Effective mass plateaux for the vector meson mass at $\mu a = 0.005$ and at $\mu a = 0.06$. Notice the different scale on the y axis.*

quantity (for example the pion mass). Then matching this universal factor with a renormalized matrix element (the bare matrix element computed in the target regularization) at the reference point and at fixed lattice spacing, it is trivial to extract the renormalization factor. Obviously the method works, using the symmetry properties of the target regularization, if it is possible to relate renormalization factors of different local operators. To this end, we have used two different matching conditions. We have matched the RGI quark mass (method 1) and the matrix element of the pseudoscalar density (method 2) (see [21] for details) at the reference points given by $x_{\text{ref}} = (r_0 M_\pi)^2 = 1.5736, 3.0, 5.0$, where the last point is considered only for twisted mass fermions (in the overlap case we do not have data in the region corresponding to such high pion masses). The universal factor was obtained using the renormalization constants and the bare matrix elements computed by the ALPHA collaboration [24, 25] using $\mathcal{O}(a)$ non-perturbatively improved Wilson fermions. For overlap fermions, due to the lattice chiral symmetry [5], we have the following relation between the renormalization factors of the pseudoscalar and scalar density and the renormalization factor of the quark mass,

$$Z_P = Z_S = \frac{1}{Z_m} . \quad (14)$$

For Wtm, due to the existence of an exact flavor symmetry for massless Wilson quarks, we obtain

$$Z_P = \frac{1}{Z_\mu} \quad (15)$$

for all the flavor components. We summarize our results in Table 4. For overlap fermions, these results are basically independent from choosing $x_{\text{ref}} = 1.5736, 3.0$. In the twisted mass case, the slight dependence (always within 1-2 standard deviations)

x_{ref}	method 1	method 2	method 1	method 2
	$Z_m^{\text{RGI,ov}}$	$Z_m^{\text{RGI,ov}}$	$Z_\mu^{\text{RGI,tm}}$	$Z_\mu^{\text{RGI,tm}}$
1.5736	1.02(6)	0.98(5)	2.27(7)	2.22(8)
3.0	0.98(7)	1.01(5)	2.32(6)	2.36(6)
5.0	–	–	2.39(5)	2.55(20)

Table 4: Results for $Z_m^{\text{RGI,ov}}$ and $Z_\mu^{\text{RGI,tm}}$.

m_{bare}^a	$m_{\text{PCAC}}^{\text{ov}a}$	$m_{\text{PCVC}}^{\text{tm}a}$
0.005	–	0.008303(7)
0.01	0.00695(2)	0.016602(8)
0.02	0.01391(3)	0.033187(17)
0.04	0.02795(5)	0.066514(24)
0.06	0.04218(6)	0.100051(35)
0.08	0.05659(7)	0.133899(42)
0.10	0.07116(8)	0.168110(51)

Table 5: *Ward identities quark masses.*

is due to the $\mathcal{O}(a^2\mu^2)$ lattice artifacts that affect the quantities used for the matching. The large error on $Z_\mu^{\text{RGI,tm}}$ at $x_{\text{ref}} = 5.0$ from method 2 comes from the error on the universal factor computed from the data of the ALPHA collaboration in the continuum limit. The rather large value of the renormalization constant in the case of Wtm fermions is reflected in the slope of the curves shown in Figures 1 and 2.

3.3 Ward identities quark masses

The Ward identities (WI) quark masses $m_{\text{PCAC}}^{\text{ov}}$ and $m_{\text{PCVC}}^{\text{tm}}$ can be extracted from the ratios

$$\begin{aligned}
m_{\text{PCAC}}^{\text{ov}} &= \frac{\sum_{\vec{x}} \langle \partial_0 A_0^\dagger(\vec{x}, x_0) P(0) \rangle}{2 \sum_{\vec{x}} \langle P^\dagger(\vec{x}, x_0) P(0) \rangle}, \\
m_{\text{PCVC}}^{\text{tm}} &= \frac{\epsilon^{3bc} \sum_{\vec{x}} \langle \partial_0 V_0^b(\vec{x}, x_0) P^c(0) \rangle}{2 \sum_{\vec{x}} \langle P^c(\vec{x}, x_0) P^c(0) \rangle}.
\end{aligned} \tag{16}$$

Results for the (WI) quark masses are reported in Table 5 and plotted in Figure 5, together with the results of a quadratic extrapolation to the chiral limit.

From the values of the WI quark masses and the bare quark masses, the corresponding renormalization factors can be computed at each value of the bare quark mass. They are then given by

$$Z_A^{\text{ov}} = \frac{m_{\text{ov}}}{m_{\text{PCAC}}^{\text{ov}}}, \quad Z_V^{\text{tm}} = \frac{\mu}{m_{\text{PCVC}}^{\text{tm}}}. \tag{17}$$

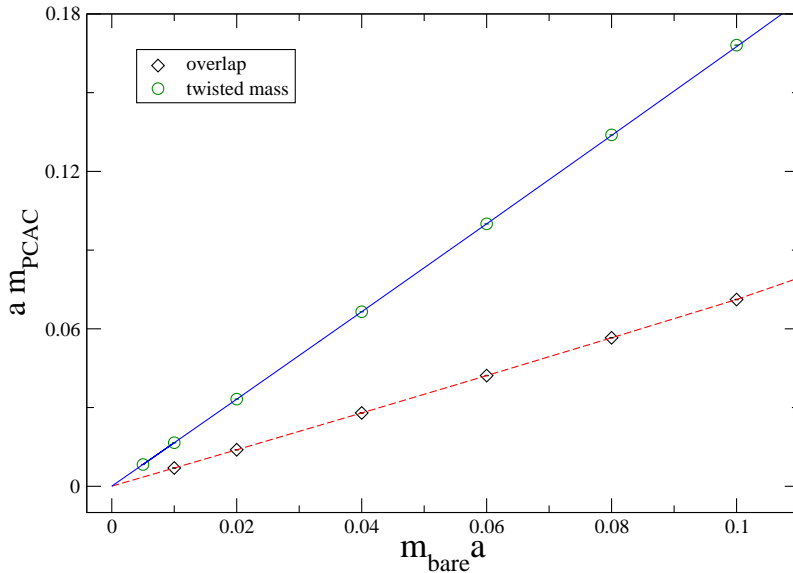


Figure 5: Comparison of results for the WI quark masses as a function of the quark mass for overlap and twisted mass fermions. The values of m_{PCAC} and m_{PCVC} extrapolated quadratically to the chiral limit are 0.00004(2) and 0.00003(1) for the overlap and the Wtm case respectively.

The behavior of the WI quark masses in Figure 5 is only apparently linear. In the overlap case this behavior is well described by a quadratic curve (where the quadratic term is quite small). This is reflected in the linear behavior of Z_A^{ov} with a rather mild slope (see Figure 6). A linear fit (excluding the data point at $am_{\text{ov}} = 0.01$) allows then to obtain a value for Z_A^{ov} in the chiral limit, $Z_A^{\text{ov}} = 1.448(4)$. In the twisted mass case even a quadratic fit is inadequate to describe the behavior of the PCVC mass with respect to the bare mass μ . This is reflected in the behavior of Z_V^{tm} as function of μ — see Figure 7 — which, in particular at small quark masses, is altered by residual lattice artifacts. This affects the denominator of Eq. (17) (i.e. $m_{\text{PCVC}}^{\text{tm}}$), giving rise to a strong non-linearity. For this reason we prefer not to quote any value for Z_V^{tm} in the chiral limit.

3.4 Pseudoscalar decay constants

The pseudoscalar decay constants can be computed from the ratios

$$f_\pi^{\text{ov}} = \frac{Z_A^{\text{ov}} |\langle 0 | A_0 | \pi \rangle_{\text{ov}}|}{M_\pi^{\text{ov}}}, \quad f_\pi^{\text{tm}} = \frac{Z_V^{\text{tm}} |\langle 0 | V_0^b | \pi \rangle_{\text{tm}}|}{M_\pi^{\text{tm}}} \quad b = 1, 2 \quad (18)$$

which require the determination of Z_A^{ov} and of Z_V^{tm} as discussed in the previous section (where at maximal twist Z_V^{tm} should be identical to the value computed with standard Wilson fermions).

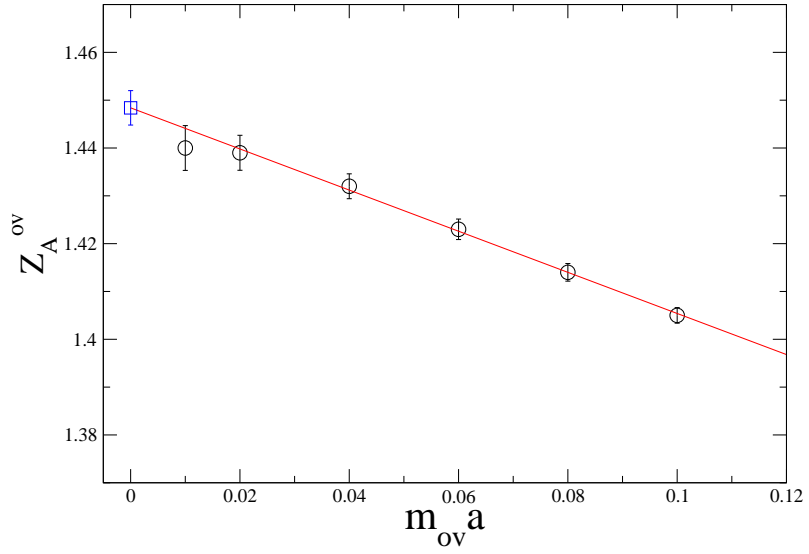


Figure 6: Z_A^{ov} as function of the quark mass and its chiral extrapolation.

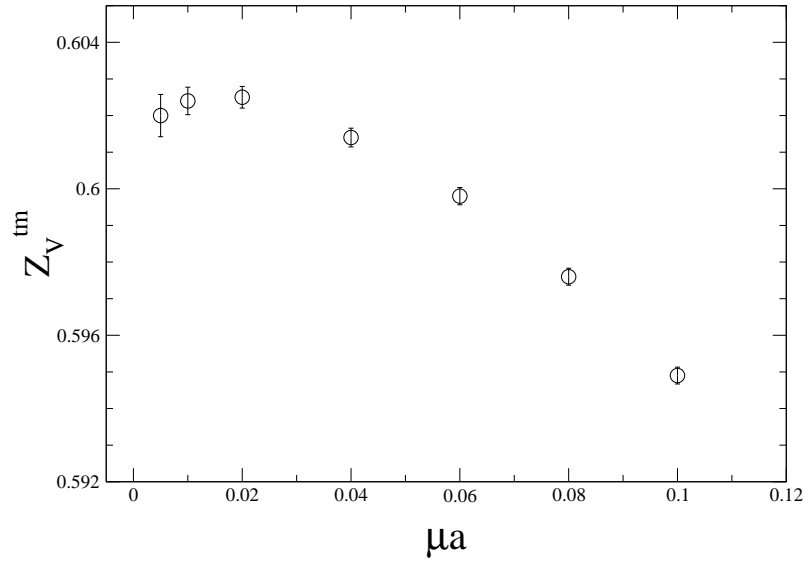


Figure 7: Z_V^{tm} as function of the quark mass.

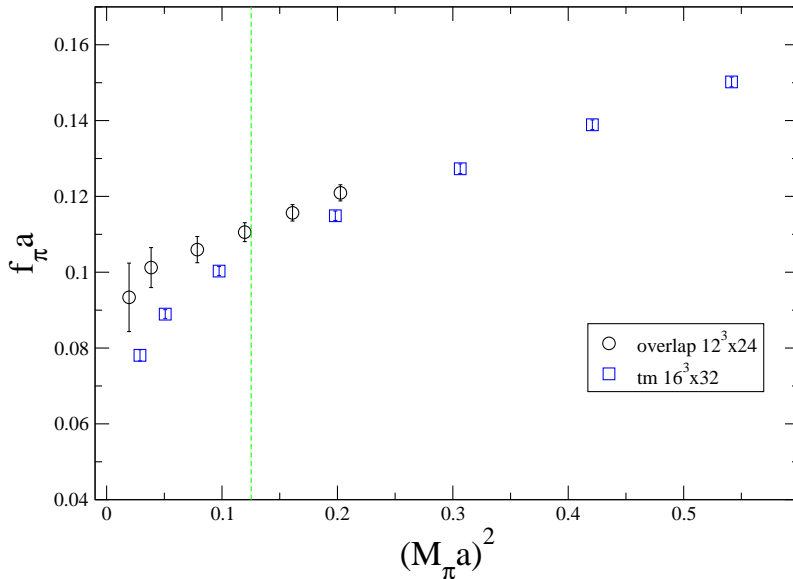


Figure 8: Comparison of results for the pion decay constant as a function of the pion mass squared for overlap and twisted mass fermions. The vertical line represents the value of $(M_\pi a)^2$ which corresponds to a bare quark mass $\bar{m}_q a = a^2 \Lambda_{\text{QCD}}^2$, i.e. the r.h.s. of Eq. (21) apart from an unknown proportionality factor.

There is also a second, “indirect” method that uses the PCAC and PCVC relations and does not require the computation of any renormalization constant,

$$f_\pi^{\text{ov}} = \frac{2m_{\text{ov}}}{(M_\pi^{\text{ov}})^2} |\langle 0 | P | \pi \rangle_{\text{ov}}|, \quad f_\pi^{\text{tm}} = \frac{2\mu}{(M_\pi^{\text{tm}})^2} |\langle 0 | P^b | \pi \rangle_{\text{tm}}|, \quad b = 1, 2. \quad (19)$$

This second method will prove to be useful especially for the Wtm case.

From the theoretical side we expect from one loop quenched chiral perturbation theory (qχPT) that f_π has neither chiral logarithms nor finite volume effects,

$$f_\pi = f \left(1 + \frac{\alpha_5}{(4\pi f)^2} M_\pi^2 \right), \quad (20)$$

where α_5 is a low energy constant.

As we have seen in the previous section, a reliable number for Z_V^{tm} cannot be provided given the strong quark mass dependence of the renormalization constant in the Wtm case. We therefore only give values for f_π from the “indirect” method. Results for the pion decay constant obtained with the “indirect” method for both overlap (from $C_{P-S, \text{ov}}(x_0)$) and twisted mass fermions (from $C_{P, \text{tm}}^b(x_0)$) are reported in Table 6 and plotted in Figure 8.

This Figure reveals that in the case of the overlap fermion f_π nicely follows the linear behavior predicted from quenched chiral perturbation theory. However, in the

$m_{\text{bare}}a$	$f_{\pi}^{\text{ov}}a$	$f_{\pi}^{\text{tm}}a$
0.005	-	0.0781(15)
0.01	0.0934(90)	0.0889(12)
0.02	0.1012(53)	0.1003(12)
0.04	0.1060(34)	0.1149(12)
0.06	0.1106(25)	0.1273(13)
0.08	0.1157(22)	0.1389(13)
0.10	0.1209(21)	0.1502(13)

Table 6: Pseudoscalar decay constants from the “indirect” method, Eqs. (19).

case of Wtm fermions we observe a *bending* of f_{π}^{tm} when the pion mass is small. It has been argued [4] that the condition

$$m_q a \gg a^2 \Lambda_{\text{QCD}}^2 \quad (21)$$

(where $m_q = \sqrt{\tilde{m}^2 + \mu^2}$ is equal to μ at full twist) has to be satisfied (with some proportionality factor in front of the r.h.s.) in order the explicit breaking of the chiral symmetry to be driven by the mass term rather than by the Wilson term (in which case large cut-off effects could appear). If this is the effect we are seeing in Figure 8, then this inequality seems to be satisfied with a proportionality constant of $\mathcal{O}(1)$. In order to visualize this, we represent the squared pion mass corresponding to a bare quark mass $\tilde{m}_q a = a^2 \Lambda_{\text{QCD}}^2$ as the vertical dotted line in Figure 8. What is puzzling is that, for a setup where the correlators are $\mathcal{O}(a)$ improved (as it should be in our simulations of Wilson twisted mass fermions), one could hope that the condition that has to be satisfied is $m_q a \gg a^3 \Lambda_{\text{QCD}}^3$ rather than the condition in Eq. (21). In this case, all of our data should be safe, unless the proportionality constants in front of the r.h.s. is a large number. Clearly the bending phenomenon observed in Figure 8 deserves further analytical and numerical investigations and can be clarified presumably only when results at smaller lattice spacings are available.

For overlap fermions, the renormalization constant can be reliably extracted in the chiral limit and hence also the “direct” method can be used. For these two methods we have considered both the simplest correlators $C_{P,\text{ov}}(x_0)$ (“indirect”) and $C_{A_0,\text{ov}}(x_0)$ (“direct”), as well as the composite ones $C_{P-S,\text{ov}}(x_0)$ (“indirect”) and $C_{A_0+V_0,\text{ov}}(x_0)$ (“direct”), where the finite volume effects from the zero modes cancel. The results in the chiral limit for the four cases turn out to be compatible within the errors,

$$\begin{aligned} \lim_{m_{\text{ov}} \rightarrow 0} f_{C_{P-S}}^{\text{ov}} a &= 0.0963(52) , \\ \lim_{m_{\text{ov}} \rightarrow 0} f_{C_P}^{\text{ov}} a &= 0.0980(46) , \\ \lim_{m_{\text{ov}} \rightarrow 0} f_{C_{A_0+V_0}}^{\text{ov}} a &= 0.1010(40) , \\ \lim_{m_{\text{ov}} \rightarrow 0} f_{C_{A_0}}^{\text{ov}} a &= 0.1018(38) . \end{aligned}$$

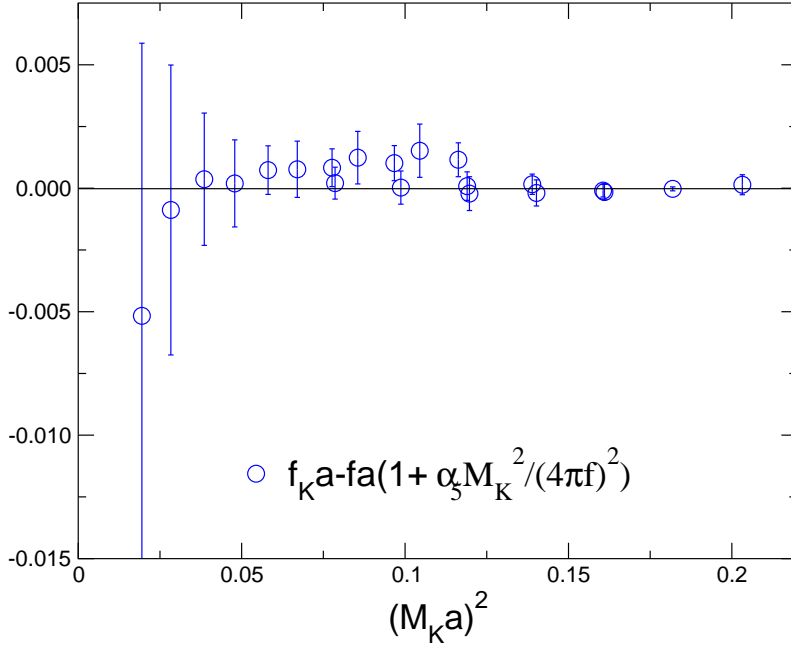


Figure 9: *Difference between the results for the decay constant and a linear fit to degenerate data only.*

This means that the finite volume effects, which in the case of $C_{P,ov}(x_0)$ and $C_{A_0,ov}(x_0)$ may affect both the pseudoscalar mass and the matrix element, cancel out when one takes the suitable ratio needed to compute f_π . The slight difference between the “direct” and the “indirect” method can be ascribed to the different $\mathcal{O}(a^2)$ lattice artifacts of the two correlators used and also to the uncertainty in the chiral extrapolation of Z_A^{ov} needed for the “direct” method.

Since for overlap fermions the behavior of f_π^{ov} is perfectly linear, as predicted by quenched chiral perturbation theory — in contrast to the Wtm case — we can hope to check the prediction of q χ PT in the case of f_K^{ov} . Moreover, since the two methods for extracting f_π are in good agreement, in the non-degenerate case we use only the PCAC method,

$$f_K^{ov} = \frac{m_{ov,1} + m_{ov,2}}{(M_K^{ov})^2} |\langle 0|P|K \rangle_{ov}|. \quad (22)$$

At one loop in q χ PT, f_K takes the form

$$f_K = f \left(1 + \frac{\alpha_5}{(4\pi f)^2} M_K^2 + \text{FV} + \text{LG} \right) \quad (23)$$

where f and α_5 are the same as in Eq. (20), “FV” are finite size effects and “LG” logarithmic corrections (see Ref. [26] for the complete formula).

One could envisage the following strategy: determine f and α_5 from the degenerate data and search for FV and LG. Unfortunately, within our statistical accuracy

we see only a linear behavior in M_K^2 , with α_5 in perfect agreement with the determination from the degenerate data (i.e. from f_π). This is displayed in Figure 9, where we plot the difference between the data and the values obtained from the q χ PT formula for f_K without the terms FV and LG and where α_5 and f are determined from the degenerate case only.

The results we get are $f_\pi = 155(11)$ MeV, $f_K = 173(8)$ MeV, $f_K/f_\pi = 1.11(3)$, $\alpha_5 = 1.85(30)$. As usual in the quenched approximation, the value of f_K/f_π turns out to be about 10% smaller than its experimental value.

3.5 Baryon masses

In order to extract baryon masses we use the following interpolating operators (for the octet and the decuplet respectively),

$$\begin{aligned} B_\alpha^{\text{oct}} &= \epsilon^{ABC} [((d^A)^T C \gamma_5 u^B) u_\alpha^C - ((u^A)^T C \gamma_5 d^B) u_\alpha^C] , \\ B_{k,\alpha}^{\text{dec}} &= \epsilon^{ABC} ((u^A)^T C \gamma_k u^B) u_\alpha^C , \quad k = 1, 2, 3 , \end{aligned} \quad (24)$$

where C is the charge conjugation matrix. For the decuplet $k = 1, 2, 3$ are equivalent. We have chosen $k = 1$.

For correlators at zero momentum in the overlap case, we have

$$\sum_{\vec{x}} (1 + \gamma_4)_{\alpha\beta} \langle \bar{B}_\alpha^{\text{oct,dec}}(\vec{x}, x_0) B_\beta^{\text{oct,dec}}(0) \rangle_{\text{ov}} \propto e^{-Mx_0} , \quad a \ll x_0 \leq \frac{T}{2} . \quad (25)$$

In this case we perform a simple exponential fit in the first half of the lattice in the time direction to avoid contaminations coming from the state with opposite parity. In the twisted mass case (at twist angle $\omega = \pi/2$) it is easy to show that

$$\langle \bar{B}_\alpha^{\text{oct,dec}}(x) B_\beta^{\text{oct,dec}}(0) \rangle_{\text{phys}} = \frac{1}{2} (1 + i\gamma_5)_{\alpha\gamma} \langle \bar{B}_\gamma^{\text{oct,dec}}(x) B_\delta^{\text{oct,dec}}(0) \rangle_{\text{tm}} (1 + i\gamma_5)_{\delta\beta} , \quad (26)$$

where $\langle \bar{B}_\alpha^{\text{oct,dec}}(x) B_\beta^{\text{oct,dec}}(0) \rangle_{\text{phys}}$ is the correlator with the correct quantum numbers in the continuum.

Results (obtained by using sink-smearing) are reported in Table 7 and plotted in Figure 10. Concerning overlap fermions, due to the relatively small volume, the decuplet channel as well as the octet correlators corresponding to the lowest two bare quark masses are too noisy and we are not able to extract the corresponding masses. In the Wtm case, we observe a bending of the data at small quark masses similar to the case of the vector meson, whereas at bare quark masses larger than 50 MeV the results seems to behave very similarly to the overlap data.

4 Conclusions

In this paper we confronted quenched simulation results of overlap fermions and Wtm fermions in their approach to the chiral limit. We emphasize that we tested

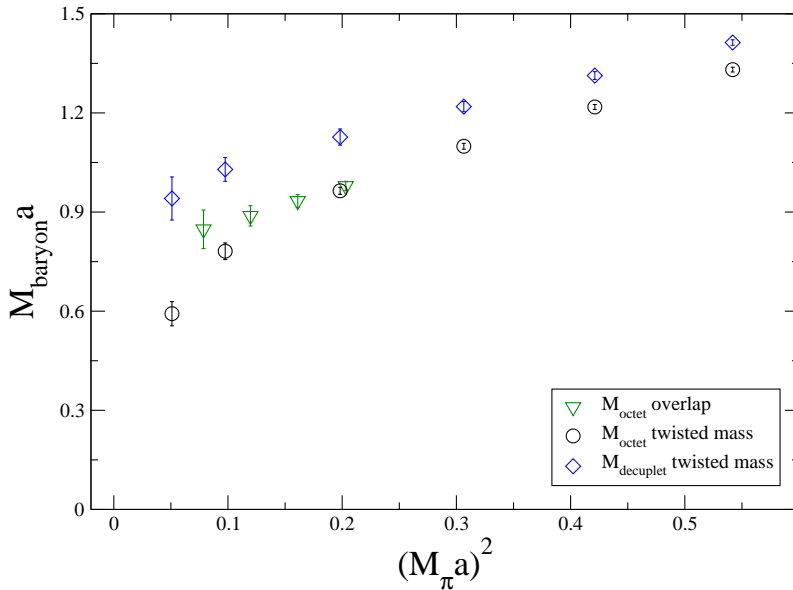


Figure 10: Comparison of results for the baryon masses (octet and decuplet in the $SU(3)$ symmetric limit) as a function of the pion mass squared for overlap and twisted mass fermions.

both lattice discretizations of QCD at only one value of $\beta = 5.85$ corresponding to a value of the lattice spacing of $a = 0.123$ fm. Although scaling tests are certainly of great importance to further explore the potential of both kind of fermions, our results show already very interesting features.

The first is that indeed with both kind of lattice fermions small values of the light meson masses can be reached, such as $M_\pi \simeq 220$ MeV in the overlap case and $M_\pi \simeq 270$ MeV in the Wtm case. In addition, the statistical fluctuations for the observables studied here are comparable for both formulations. This is very promising. In a detailed algorithmic study [9] we find that Wilson twisted mass fermions are a factor of 20 to 40 faster than overlap fermions. Thus Wilson twisted mass fermions have the potential for dynamical fermions simulations at realistically small quark masses on the next generation of supercomputers in the multi-teraflops range.

However, we believe that a number of questions have to be addressed to understand better the Wtm formulation of lattice QCD: In the quenched comparison of overlap and Wilson twisted mass fermions, we encountered a “*bending*” phenomenon for Wtm fermions. This effect manifests itself in the chiral approach of all the quantities studied here. While the data for overlap fermions extrapolate nicely linearly, the data for Wtm fermions show a bending when the quark mass assumes too small values. This effect might be explained by the interplay of the Wilson term and the twisted mass term, which requires one of the two inequalities discussed in Sec. 3.4

$m_{\text{bare}}a$	$M_{\text{octet}}^{\text{ov}}a$	$M_{\text{octet}}^{\text{tm}}a$	$M_{\text{decuplet}}^{\text{tm}}a$
0.01	-	0.592(37)	0.941(65)
0.02	-	0.782(25)	1.029(36)
0.04	0.8479(58)	0.963(11)	1.126(25)
0.06	0.8885(31)	1.0987(88)	1.2199(15)
0.08	0.9336(19)	1.2183(74)	1.3124(12)
0.10	0.9788(14)	1.3302(72)	1.4136(83)

Table 7: Baryon masses with sink smearing.

to be satisfied.

For the present simulations at only one value of the lattice spacing we are not able to determine the cause of this “bending” phenomenon and whether it disappears in the continuum limit. For this, a detailed scaling analysis would be necessary, a work that is in progress. Overlap fermions on the other hand nicely approach the chiral limit close to the physical point with realistic light meson masses. It seems that the conceptual virtues of this approach become more and more important, the smaller the quark mass is chosen. However, we believe that a final answer, which formulation to use for extracting physics in the chiral limit, can only be given when the scaling behavior of both approaches is understood.

For dynamical simulations the presence of a first order phase transition has been seen for Wtm fermions [10]. This observation is in accordance with an effective potential picture [27, 28, 29, 22]. The findings in Ref. [10] just emphasize the fact that the study of the phase structure of lattice QCD is a necessary prerequisite for reliable physics results.


Acknowledgments

We are indebted to R. Frezzotti and G. C. Rossi for many useful remarks and suggestions. We thank also M. Müller-Preußker for useful discussions. The computer centers at NIC/DESY Zeuthen, NIC at the Forschungszentrum Jülich and HLRN provided the necessary technical help and the computer resources. We thank the staff of these centers for their help and advise. This work was supported by the DFG Sonderforschungsbereich/Transregio SFB/TR9-03.

References

- [1] S. Weinberg, *Physica* **A96** (1979) 327.
 J. Gasser and H. Leutwyler, *Ann. Phys. (N.Y.)* **158** (1984) 142.
 J. Gasser and H. Leutwyler, *Phys. Lett.* **B184** (1987) 83.

- [2] H. Neuberger, Phys. Lett. **B417** (1998) 141; hep-lat/9707022. Phys. Lett. **B427** (1998) 353; hep-lat/9801031.
- [3] R. Frezzotti, P.A. Grassi, S. Sint and P. Weisz, Nucl. Phys. B (Proc. Suppl.) **83** (2000) 941; JHEP **0108** (2001) 058; hep-lat/0101001.
- [4] R. Frezzotti and G.C. Rossi, JHEP **0408** (2004) 007, Nucl. Phys. B (Proc. Suppl.) **128** (2004) 193; hep-lat/0311008.
- [5] M. Lüscher, Phys. Lett. **B428** (1998) 342; hep-lat/9802011.
- [6] P. Hasenfratz, V. Laliena and F. Niedermayer, Phys. Lett. **B427** (1998) 317; hep-lat/9801021. P. Hasenfratz, Nucl. Phys. **B525** (1998) 401; hep-lat/9802007.
- [7] L. Giusti, C. Hoelbling and C. Rebbi, Phys. Rev. **D64** (2001) 114508; Erratum-ibid. **D65** (2002) 079903; hep-lat/0108007. F. Berruto, N. Garron, C. Hoelbling, J. Howard, L. Lellouch, S. Necco, C. Rebbi and N. Shoresh, hep-lat/0409132. Y. Chen, S.J. Dong, T. Draper, I. Horváth, F.X. Lee, K.F. Liu, N. Mathur and J.B. Zhang, Phys. Rev. **D70** (2004) 03450; hep-lat/0304005.
- [8] χ L^F Collaboration: K. Jansen, A. Shindler, C. Urbach and I. Wetzorke, Phys. Lett. **B586** (2004) 432; hep-lat/0312013.
- [9] χ L^F Collaboration: T. Chiarappa, K. Jansen, K.-I. Nagai, M. Papinutto, L. Scorzato, A. Shindler, C. Urbach, U. Wenger and I. Wetzorke, hep-lat/0409107 and in preparation.
- [10] F. Farchioni, R. Frezzotti, K. Jansen, I. Montvay, G.C. Rossi, E. Scholz, A. Shindler, N. Ukita, C. Urbach and I. Wetzorke, hep-lat/0406039; hep-lat/0409098.
- [11] F. Niedermayer, Nucl. Phys. B (Proc. Suppl.) **73** (1999) 105; hep-lat/9810026. P. Hernández, Nucl. Phys. B (Proc. Suppl.) **106** (2002) 80; hep-lat/0110218. S. Chandrasekharan and U.-J. Wiese, Prog. Part. Nucl. Phys. **53** (2004) 373.
- [12] R. Frezzotti, hep-lat/0409138.
- [13] P.H. Ginsparg and K.G. Wilson, Phys. Rev. **D25** (1982) 2649.
- [14] R. Sommer, Nucl. Phys. **B411** (1994) 839; hep-lat/9310022. M. Guagnelli, R. Sommer and H. Wittig, Nucl. Phys. **B535** (1998) 389; hep-lat/9806005.
- [15] R.W. Freund, in *Numerical Linear Algebra*, L. Reichel, A. Ruttan and R.S. Varga (eds.), Berlin 1993, p. 101. U. Gläsner, S. Güsken, Th. Lippert, G. Ritzenhöfer, K. Schilling and A. Frommer, hep-lat/9605008. B. Jegerlehner, hep-lat/9612014, Nucl. Phys. B (Proc. Suppl.) **63** (1998) 958; hep-lat/9708029.

- [16] R. M. Baxter, Ph.D. Thesis, Chapter 3, Edinburgh 1993.
- [17] UKQCD Collaboration: C. R. Allton *et al.*, Phys. Rev. **D47** (1993) 5128; hep-lat/9303009.
- [18] T. Blum *et al.*, Phys. Rev. **D69** (2004) 074502; hep-lat/0007038.
S. J. Dong *et al.*, Phys. Rev. **D65** (2002) 054507; hep-lat/0108020. BGR Collaboration: C. Gattringer *et al.*, Nucl. Phys. **B677** (2004) 3; hep-lat/0307013.
- [19] ZeRo Collaboration: M. Guagnelli *et al.*, Phys. Lett. **B597** (2004) 216; hep-lat/0403009.
- [20] P. Hernández, K. Jansen, L. Lellouch and H. Wittig, JHEP **0107** (2001) 018; hep-lat/0106011.
- [21] P. Hernández, K. Jansen, L. Lellouch and H. Wittig, Nucl. Phys. B (Proc. Suppl.) **106** (2002) 766; hep-lat/0110199.
- [22] L. Scorzato, hep-lat/0407023.
- [23]  Collaboration, in progress.
- [24] S. Capitani, M. Lüscher, R. Sommer and H. Wittig, Nucl. Phys. **B544** (1999) 669; hep-lat/9810063.
- [25] J. Garden, J. Heitger, R. Sommer and H. Wittig, Nucl. Phys. **B571** (2000) 237; hep-lat/9906013.
- [26] D. Bećirević and G. Villadoro, Phys. Rev. **D69** (2004) 054010; hep-lat/0311028.
- [27] S.R. Sharpe and R. Singleton, Phys. Rev. **D58** (1998) 074501; hep-lat/9804028.
- [28] G. Münster, JHEP **0409**, 035 (2004); hep-lat/0407006.
- [29] S. R. Sharpe and J. M. S. Wu, hep-lat/0407025.